Mineralogical Magazine, October 2016, Vol. 80(6), pp. 1041–1053

Isoferroplatinum-pyrrhotite-troilite intergrowth as evidence of desulfurization in the Merensky Reef at Rustenburg (western Bushveld Complex, South Africa)

Alexander Kawohl[1,*] and Hartwig E. Frimmel[1,2]

[1] Institute of Geography and Geology, University of Würzburg, Am Hubland D-97074, Würzburg, Germany
[2] Department of Geological Sciences, University of Cape Town, Rondebosch 7700, South Africa

[*Received 30 July 2015; Accepted 4 November 2015; Associate Editor: Brian O'Driscoll*]

ABSTRACT

Petrographic and mineralogical studies of samples of the Normal (or undisturbed) Merensky Reef from Frank Shaft No.1 at Rustenburg Platinum Mine revealed the presence of a Pt-Fe-alloy, probably isoferroplatinum (58 vol.% of total precious metal minerals), arsenides (21 vol.%), bismuthotellurides (10 vol.%), electrum (9 vol.%) and platinum group element- (PGE-) sulfides and stannides (2 vol.%), associated predominantly with base-metal- and iron-sulfides. A Pt-Fe-alloy-dominated facies has been known for considerable time from potholes and discordant bodies and has been attributed to fluid activity with high f_{O_2} and low f_{S_2}. Our petrographic results indicate that the normal thin reef has also undergone hydrothermal alteration. For the first time, the rare mineral troilite (stoichiometric FeS) was found as intergrowths with masses of Pt-Fe-alloy, together with Fe-rich pyrrhotite, secondary hydrous silicates, magnetite and calcite. The observed mineral assemblage and texture is interpreted as the product of partial desulfurization, caused by migrating S-undersaturated fluids, which led to the exsolution of Pt-Fe-alloy from pyrrhotite ($Fe_{x-1}S$) with the latter approaching a stoichiometric composition. Overall our new observations provide convincing support for the importance of metasomatism in the secondary modification of ore mineralogy and textures even in the undisturbed Merensky Reef.

Keywords: Merensky Reef, Bushveld Complex, platinum-group minerals, troilite, isoferroplatinum, Pt-Fe-alloy, desulfurization.

Introduction

The Merensky Reef, a thin and laterally extensive platinum-group element (PGE)-Ni-Cu ore body in South Africa's world famous Bushveld Igneous Complex averages at normal mining thickness (~90 cm) 5.0–9.0 ppm PGE + Au, including c. 3.0–4.0 ppm Pt and 1.5–2.0 ppm Pd (Lee, 1996; Cawthorn *et al.*, 2005). The PGE and Au are both hosted as solid solution in bisulfides, such as pentlandite, pyrrhotite and chalcopyrite, and occur also as small (nm to tens-of-µm sized) discrete phases, that is platinum-group minerals (PGM) (e.g. Osbahr *et al.*, 2013; Junge *et al.*, 2015). While PGE proportions and ore grades of the reef are nearly constant along the whole Bushveld Complex, the PGM assemblages are, even at a local scale, highly variable. Information about the precious metal minerals, their composition, size, distribution and association, can not only contribute to the debate about the still poorly understood genesis of this style of mineralization but is also of considerable metallurgical importance for ore processing.

Numerous genetic models have been suggested to explain the Merensky Reef, including the following: (1) leaching of the cumulate pile, redistribution and upgrading of PGE concentrations by ascending late-stage magmatic Cl-bearing fluids (e.g. Ballhaus and Stumpfl, 1986; Boudreau and

*E-mail: alex.kawohl@yahoo.de
DOI: 10.1180/minmag.2016.080.055

McCallum, 1992; Boudreau and Meurer, 1999; Willmore *et al.*, 2000); (2) exsolution of immiscible sulfide melt droplets, caused by wall-/roof-rock assimilation, magma mixing, pressure fluctuations or Fe-fractionation, all of which concentrate PGE from the magma into the cumulate (e.g. Campbell *et al.*, 1983; Naldrett and von Gruenewaldt, 1989; Schönberg *et al.*, 1999; Cawthorn, 2005, 2010); (3) direct crystallization and precipitation of PGM or PGE clusters from the magma (e.g. Hiemstra, 1979; Merkle, 1992; Tredoux *et al.*, 1995; Ballhaus and Sylvester, 2000; Helmy *et al.*, 2013); (4) processes of PGE pre-concentration and crystallization in a staging chamber beneath the Bushveld Complex or in feeders, followed by the intrusion of a PGE-enriched crystal mush into the Rustenburg Layered Suite (Naldrett *et al.*, 2009; Hutchinson *et al.*, 2015 and references therein); and (5) hydrodynamic sorting of sulfides, PGM, silicates and oxides during subsidence-induced mobilization of semi-consolidated cumulates (Maier *et al.*, 2013). In addition to the various hypotheses to explain the primary origin of the reef, numerous other processes have been suggested to account for the nature and variability of discrete PGM, from direct crystallization of PGE clusters (e.g. Tredoux *et al.*, 1995) or laurite (e.g. Merkle, 1992; Finnigan *et al.*, 2008), to subsolidus re-equilibration and exsolution of PGM from base metal and Fe-sulfides (e.g. Ballhaus and Ryan, 1995), to high-*T* fractionation of semimetal-PGE-liquids from a sulfide melt (Helmy *et al.*, 2007; Holwell and McDonald, 2010) and other processes involving desulfurization (e.g. Peregoedova *et al.*, 2004; Li and Ripley, 2006).

The role and significance of fluids in the formation of the ores has been a highly contentious issue. The notion of considerable hydrothermal modification and redistribution of chalcophile and siderophile elements in the Bushveld Complex has repeatedly been challenged (see reviews by Cawthorn, 1999, 2010; Barnes and Maier, 2002; Godel *et al.*, 2007). Nevertheless, more recently the role and importance of fluids in the PGE-metallogenesis in layered intrusions has been emphasized, e.g. by Li *et al.* (2004, 2008), Li and Ripley (2006), Boudreau (2008), Godel and Barnes (2008), and Kanitpanyacharoen and Boudreau (2013). The objective of this study is to contribute to this discussion on the basis of detailed analyses of the texture and mineralogy of the ore and gangue minerals in the 'normal' (or undisturbed) facies of the Merensky Reef, i.e. the reef facies that has been traditionally considered least affected by fluid-rock interaction.

Geological background

The 2.055–2.056 Ga old Bushveld Igneous Complex extends over some 350 km × 450 km on surface and subsurface in the northeast of the Republic of South Africa, north of the cities of Johannesburg and Pretoria. According to the definition given by SACS (1980), the Bushveld Complex comprises four stratigraphic subdivisions: The Rashoop Granophyre and the Lebowa Granite suites, the Rooiberg Group volcanic rocks, as well as the 6–8 km thick (ultra-)mafic Rustenburg Layered Suite (RLS). This layered series, having an elliptical-shaped (Fig. 1*a*) outcrop (subcrop) of some 65,000 km^2, represents the largest layered intrusion on Earth and is characterized by a distinctive, partly-rhythmical igneous layering of dunite, harzburgite, norite, gabbro, anorthosite and chromitite. On the basis of major lithological changes, the RLS has been traditionally subdivided into a number of zones (Fig. 1*b*): The Marginal Zone (0–800 m thick) comprises unlayered norite cumulates in contact to the metasedimentary host rocks, overlain by a harzburgitic-dunitic Lower Zone (800–1300 m). The Critical Zone (1300–1800 m thick) includes distinctive cyclic units and 13 major chromitite seams. It is further subdivided into a Lower Critical (mainly pyroxenite) and Upper Critical Zone (mainly norite and anorthosite). The Main Zone (3000–3400 m) is of gabbronoritic composition, lacks visible igneous layering and is overlain by the Upper Zone (2000–2800 m thick). The latter comprises well-layered ferro-gabbronorite, anorthosite and several Ti-V-rich magnetite layers. The whole sequence is capped by the Rashoop Granophyre Suite. For detailed insights into the geology, stratigraphy and mineralization of the RLS, the reader is referred to Eales and Cawthorn (1996), Lee (1996), Cawthorn *et al.* (2005), Kruger (2005), Naldrett *et al.* (2011) and Maier *et al.* (2013).

The Bushveld Complex was emplaced during a short interval of approximately <100,000 years (Cawthorn and Walraven, 1998) from multiple magma additions (e.g. Kruger, 2005), possibly linked to a mantle plume (Hatton, 1995) and/or a back-arc extension (Willmore *et al.*, 2002), into the volcano-sedimentary succession of the Transvaal Supergroup within the Kaapvaal Craton. Solidification proceeded during only a

https://doi.org/10.1180/minmag.2016.080.055 Published online by Cambridge University Press

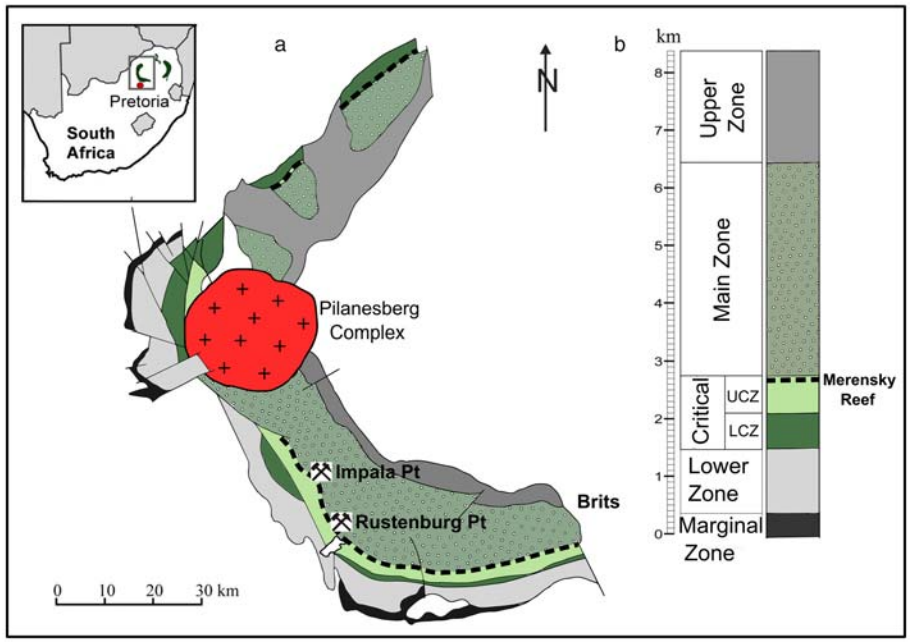

FIG. 1. (*a*) Simplified geological map of the western limb of the Bushveld Igneous Complex with the Rustenburg sample locality and outcrop of the Merensky Reef outlined in black; (*b*) generalised stratigraphy of the Rustenburg Layered Suite (modified after Godel *et al.*, 2007).

few hundred thousand years and the recent exposure of this sill-like lopolithic body at four interconnected (Webb *et al.*, 2011) lobes (Fig. 1*a*) that dip gently towards a common centre (Kruger, 2005), is believed to be the result of late-magmatic subsidence (Letts *et al.*, 2009; Cawthorn and Webb, 2013; Zeh *et al.*, 2015).

In particular the RLS is not only of scientific but also of outstanding economic interest, as it contains 95% of total PGE reserves and, respectively, 75%, 52% and 82% of the reported resources of Pt, Pd and Rh, the globally most important source of these precious metals (Naldrett *et al.*, 2008; US Geological Survey, 2015). Additionally the RLS also hosts the world's largest known resources of Cr and V. Three ore bodies are currently being mined for PGE, namely the Upper Group 2 Chromitite (UG2), the Merensky Reef and the Platreef. The complex also hosts significant amounts of other metallic resources, such as Au, Ag, Ni, Cu, Co, Fe, Ti and Sn, as well as industrial minerals (dimension stone, andalusite, asbestos) (Lee, 1996).

The 2056.1 ± 0.7 Ma to 2055.3 ± 0.6 Ma Merensky Reef (Scoates *et al.*, 2011) is, after the adjacent UG2, the largest PGE deposit known so far. It can be classified as an orthocumulate that was modified by hydrothermal alteration, deformation, post-cumulus growth and recrystallization. The ore deposit represents a stratiform, silicate-bound PGE-Ni-Cu-mineralization at the Critical Zone–Main Zone boundary, c. 2–3 km above the basal contact of the RLS (Fig. 1*b*), and 15 to 400 m above the stratiform UG2 layer. The ore body is, although variable, of lateral and down-dip continuity (Fig 1*a*) but is, in places, disturbed by so-called potholes (up to ~15 m deep, circular and also mineralized depressions with diameters that range from metres to kilometres). Broadly speaking, the Merensky Reef (i.e. the mineralized part of the Merensky Cyclic Unit) comprises a number of layers, usually with a <1 cm to several tens-of-cm-thick undulating lower chromite stringer that rests on anorthosite or norite, overlain by a feldspathic pyroxenite, harzburgite or dunite, sandwiched between another chromite seam (Lee, 1996; Naldrett *et al.*, 2009, 2011). In places, a third chromite layer is present and the whole sequence is capped by a noritic hanging wall, which finally merges upwards into anorthosite, as a part of another unmineralized cyclic unit (called the 'Bastard Unit'). The coarse-

https://doi.org/10.1180/minmag.2016.080.055 Published online by Cambridge University Press

grained to pegmatoidal texture of feldspathic pyroxenite in between the chromitite layers is a common feature in the southwestern Bushveld Complex (cf. Naldrett *et al.*, 2009, 2011; Fig. 2) and originated either from the annealing of non-pegmatoidal cumulates due to pressure fluctuations, the addition of a superheated melt (Cawthorn and Boerst, 2006), or fluid-induced flux-melting and coarsening (e.g. Boudreau, 2008). Sulfides (mainly pyrrhotite, chalcopyrite, pentlandite) are present at 2–3 vol.% as intercumulus minerals. The highest PGE concentrations are observed in the vicinity of chromite layers, correlate with the sulfide mineralization, and are a function of reef thickness.

As illustrated in Fig. 2, a variety of different facies types of the Merensky Reef can be distinguished, the most important of which are listed below. For the southwestern part of the Bushveld, the vertical separation of the upper and lower chromite layer decreases from southeast (near Brits) to northwest (south to the Pilanesberg Complex, see Fig. 1*a*). At the Impala Mine (Fig. 1*a*), the so-called 'contact reef' comprises two superimposed chromite stringers and sulfide mineralization continues into the footwall. The pre-Merensky pyroxenite in between thickens southeastwards. At Rustenburg (Fig. 1*a*), the chromitite layers are each ~1 cm thick and the pegmatoidal pyroxenite ranges from <10 cm ('thin reef') up to 60 cm ('wide reef') (Viljoen and Hieber, 1986). Further to the southeast (near the town Brits), the vertical separation attains >10 m with dramatically decreasing ore grades. An upper chromitite is only locally present (Naldrett *et al.*, 2009). In the western part of Rustenburg Platinum Mines, the so-called 'rolling reef' type dominates and describes an abundance of shallow potholes.

Analytical methods

This study is based on six historic hand specimens of the ~10 cm thick pegmatoidal Merensky Reef, generally referred to as the Rustenburg 'thin reef' facies or Normal Merensky Reef facies, including its ~1 cm thick chromite stringers, as well as one sample of the noritic hanging wall, all of which were collected in the 1970's at Rustenburg Mine (Frank Shaft No.1). After petrographic analyses, the samples were further investigated by electron microprobe (EMP) using a JEOL JXA 8800L superprobe at the Department of Geodynamics and Geomaterials Research, Institute of Geography and Geology, University of Wuerzburg. The instrument is equipped with four wavelength-dispersive spectrometers. All measurements were carried out at 15 kV acceleration voltage and 20 nA beam current[§]. Scanning for PGM and native gold was carried out according to the recommendations by Xiao and Laplante (2004) and Rose *et al.* (2011) with roughly 300-fold magnification, high contrast setting and low brightness in back-scattered electron (BSE) imagining mode. Due to their large average atomic number, PGM and gold show up in strong contrast to the dark gangue. Minerals smaller than 1 μm in diameter could not be detected in BSE images. All identified precious metal minerals were logged and their grain size, expressed as equivalent circle diameter (ECD), was calculated after $ECD = 2 \times \sqrt{area/\pi}$ from their measured area in the BSE image. The PGM analytical results are only qualitative because of the small grain size, sub-microscopic intergrowths, and probable contamination by surrounding matrix. The PGE concentrations of the analysed sulfides were found to be below the lower detection limit of 0.05 wt.%. Silicates, sulfides and chromite were analysed quantitatively using the *ZAF* matrix correction procedure.

Results

Gangue minerals

Orthopyroxene ($En_{76.6}$ to $En_{84.5}$) is with 60–75 vol.% by far the dominant constituent in all layers (except the footwall). The mostly rounded-to-subhedral grains are between 2 mm and 1 cm in size and largely altered to secondary hydrous silicates and oxides. They are smaller, unaltered and of euhedral habit in the melanoritic hanging wall. Olivine (Fo_{82} to Fo_{84}; 0.36 ± 1.3 wt.% NiO) occurs as inclusions of up to 1 cm in diameter in orthopyroxene. Plagioclase and chain-like arrangements of euhedral chromite grains are also present as inclusions in orthopyroxene. Clinopyroxene occurs as pigeonite, augite and diopside ($Ca_6Mg_{78}Fe_{16}$ to $Ca_{47}Mg_{45}Fe_8$, #Mg 80–86, Al_2O_3 max. 5.5 wt.%, TiO_2 max. 1.4 wt.%, Cr_2O_3 max. 1.1 wt.%). The modal proportion is <5 vol.% and it is observed either as parallel or bleb-like exsolution lamellae in orthopyroxene or as larger, anhedral oikocrysts enclosing orthopyroxene. Plagioclase is the main felsic phase (10–20 vol.%) and shows both laterally and vertically unsystematic

[§]For further details on the instrument set-up see http://www.geodynamik.geographie.uni-wuerzburg.de/geodynamik_und_geomaterialforschung/analytische_ausstattung/elektronenstrahl_mikrosonde/

https://doi.org/10.1180/minmag.2016.080.055 Published online by Cambridge University Press

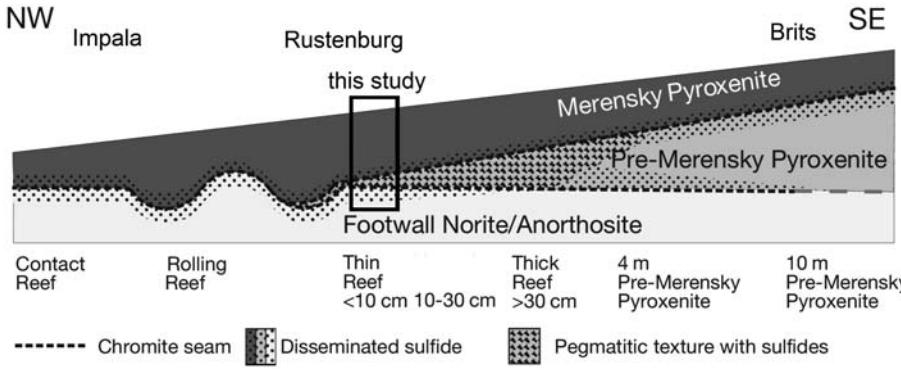

FIG. 2. Schematic cross section through the Merensky Reef in the southwestern Bushveld Complex, from Impala Mines (NW) to Eastern Platinum Mines (SE) showing the different facies types. The samples investigated are from Rustenburg thin reef facies (modified from Naldrett *et al.*, 2011).

variation in its composition, ranging from $An_{52.6}$ to $An_{75.4}$ (average An_{69}). Plagioclase has undergone moderate saussuritization and sericitization along cleavage planes and fractures and is light greenish in hand specimen. Furthermore, anhedral interstitial and Cl-bearing Ti-rich phlogopite, $(K_{1.4}(Mg_{4.3}Fe_{1.0}Al_{0.2}Ti_{0.4})[Al_{2.2}Si_{5.8}O_{20}](Cl,OH)_4)$, was noted as an accessory phase in all samples, always associated with sulfides, in places enclosing pyroxene or rutile. Alteration features (5–30 vol.%) include large (>5 mm) domains of serpentine and magnetite; fragmented sulfide aggregates (mainly chalcopyrite); calcite (up to 1 mm in size) with deformation twins; Fe-Mg carbonates; as well as fine-grained felted or tuft-like talc aggregates and sulfides that are replaced by calcic amphiboles. In contrast, phlogopite and chromite seem to be unaffected by replacement reactions and the hanging wall appears entirely unaltered. Chromite shows little variation in composition, on average (n = 47) $(Fe^{2+}_{0.74}Mg_{0.22})(Cr_{1.10}Al_{0.48}Fe^{3+}_{0.41})O_4$. Two morphological types of this spinel were observed: >2 mm large sintered or 'amoebidal' (Vukmanovic *et al.*, 2013) grains in the lower chromitite and euhedral (octahedral, 0.15 mm large) grains both in the lower and upper chromitite. Rutile and phologopite were noted as inclusions in anhedral chromite crystals of the lower chromite seam.

Sulfides

Disseminated sulfides (~50% pyrrhotite, ~30% pentlandite, ~20% chalcopyrite) are present at 0.5–3 vol.% and occur as zoned networks from a few μm to over 2 cm in size, usually with a core of pyrrhotite, surrounded by other sulfides, or at the margins replaced by alteration products (actinolite –tremolite, oxides). Many of the sulfide aggregates display fringe-like grain boundaries (Fig. 3*a*, *c*,*d*). Galena (PbS) and clausthalite (PbSe), are present as rare finely-dispersed grains, pyrite as veins through sulfides in the hanging wall. Troilite (FeS) was observed in BSE images as brighter, narrow exsolution lamellae in relatively Fe-rich pyrrhotite (Fig. 3*a*,*b*), in places chevron-like, and is distinguished from Fe-rich pyrrhotite under reflected light by its more reddish-brownish colour. This mineral, which is typically known from meteorites, is actually not very rare as a terrestrial sulfide but has been mentioned in only a few studies on the Bushveld Complex (e.g. Vermaak and Hendriks, 1976; Kinloch and Peyerl, 1990; Schouwstra *et al.*, 2000; Scoon and Mitchell, 2011). The Fe and S contents in troilite range from 62.1 to 64.2 wt.% and 35.4 to 37.3 wt.%, respectively, and the Ni content is <0.15 wt.% (Table 1). The calculated formula ranges from approximately $Fe_{51}S_{49}$ to $Fe_{49}S_{51}$. Troilite was not observed in the hanging wall. Representative compositions of sulfides are provided in Table 1.

Precious metal minerals

The modal proportions of detected precious metal minerals (n = 508), whose average size and standard deviation is 7.9 ± 8.0 μm and median size is 5.1 μm, are as follows: 57.5 vol.% isoferroplatinum, 21.0 vol.% sperrylite, 10.0 vol.% bismuthotellurides, 9.0 vol.% electrum, 1.0 vol.% laurite, 1.0 vol.% rustenburgite, and traces of cooperite,

https://doi.org/10.1180/minmag.2016.080.055 Published online by Cambridge University Press

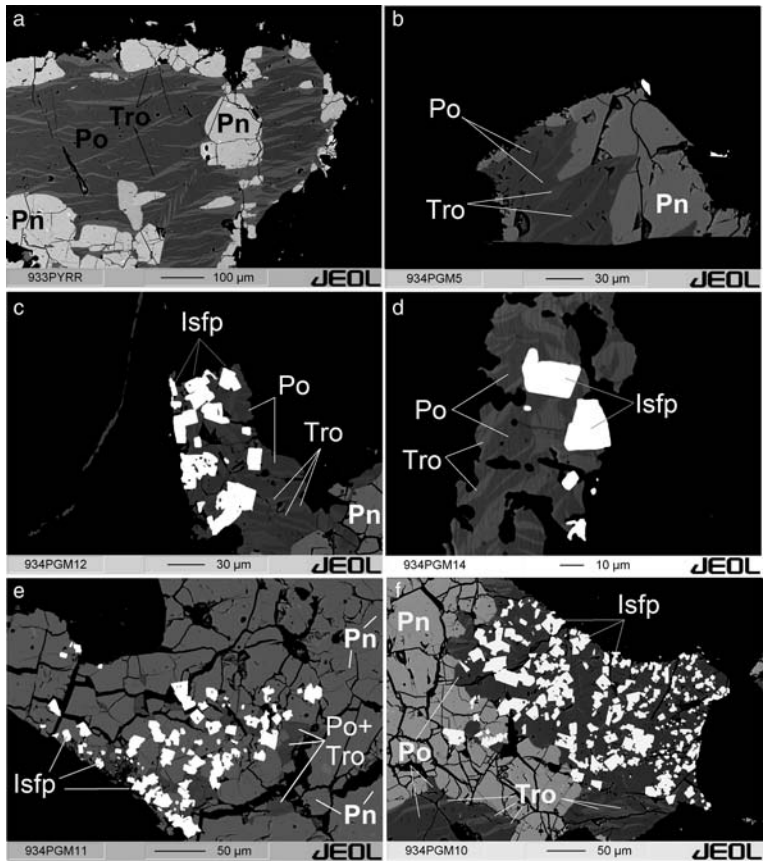

FIG. 3. Backscattered electron images of isoferroplatinum (Isfp, white), intergrown with Fe-rich pyrrhotite (Po), exsolutions flames of troilite (Tro) and mosaic-like pentlandite (Pn), in contact with gangue minerals (black). Note the preferred association of isoferroplatinum with pyrrhotite rather than with pentlandite in Fig. 3*f*.

braggite and erlichmanite All PGM occur adjacent to sulfide aggregates, even where they are entirely enclosed by silicates. Cooperite (PtS) and braggite ((Pt,Pd,Ni)S) both occur as relatively rare but large rotund grains, on average 8.0 ± 6.4 µm and 5.3 ± 4.5 µm, respectively, in size. They are preferentially associated with pentlandite and chalcopyrite. Cooperite and braggite are located typically at the contact between those sulfides and both primary (pyroxene, plagioclase) and secondary silicates (talc, chlorite). Sperrylite with the composition $PtAs_2$ occurs, in contrast to most other PGM, as unusually large, partly cracked or fragmented, rounded to angular grains with a mean ECD of 18.1 ± 16.6 µm. One grain was found to cover an area of 87 × 47 µm. This arsenide shows a strong spatial affinity to chalcopyrite and is never associated with pentlandite or pyrrhotite. Two observed grains with detectable amounts of Pb could be either sperrylite with submicroscopic intergrowths of galena or with some Pb incorporated in the sperrylite crystal structure. Alternatively it could be a sub-variety of palarstanide, $(Pd,Pt)_8(Sn, As, Pb)_3$. Laurite, $(Ru, Os, Ir)S_2$, forms a complete solid-solution series with erlichmanite, OsS_2, and was observed in minimal quantities almost entirely enclosed by pentlandite in all samples. The mineral is only rarely located at the contact between chalcopyrite and silicates and never associated with pyrrhotite. Laurite grains are small in size (on average 5.3 ± 4.1 µm), rarely euhedral (rhombic) but more commonly of needle-like habit. The few grains of erlichmanite observed are, on average, 2.8 ± 0.7 µm in ECD and located at the chalcopyrite-silicate interface. On the basis of the X-ray spectra, it cannot be determined whether

https://doi.org/10.1180/minmag.2016.080.055 Published online by Cambridge University Press

TABLE 1. Representative compositions of sulfides in the Merensky Reef.

Sulfide	S (wt.%)	Fe (wt.%)	Cu (wt.%)	Ni (wt.%)	Co (wt.%)	Total
Troilite	35.37	64.18	0.02	0.07	<0.01	99.63
Troilite	35.95	63.47	0.01	<0.01	<0.01	99.44
Troilite	37.25	62.24	<0.01	0.15	<0.01	99.64
Troilite	36.94	62.12	0.01	0.07	<0.01	99.13
Pyrrhotite	38.21	59.78	<0.01	0.32	<0.01	98.31
Pyrrhotite	36.88	61.12	<0.01	0.31	<0.01	98.30
Pyrrhotite	35.42	62.53	0.01	<0.01	<0.01	97.97
Pyrrhotite	37.82	59.68	0.01	0.04	0.33	97.88
Pentlandite	32.25	31.09	0.03	34.93	0.30	98.59
Pentlandite	32.41	33.14	0.02	33.00	0.53	99.09
Pentlandite	32.12	31.20	0.03	35.50	0.35	99.19
Pentlandite	31.98	33.77	<0.01	33.08	0.84	99.67
Pentlandite	32.29	31.40	<0.01	35.64	0.55	99.88
Pyrite	51.86	43.79	0.06	0.26	2.44	98.40
Chalcopyrite	32.96	30.93	33.35	0.05	<0.01	97.29
Chalcopyrite	33.79	30.32	33.37	0.02	<0.01	97.50
Chalcopyrite	33.57	30.82	33.53	<0.01	<0.01	97.92
Chalcopyrite	33.47	30.49	33.65	0.04	<0.01	97.65
Chalcopyrite	33.52	30.81	33.32	<0.01	<0.01	97.65
Chalcopyrite	33.91	30.81	33.15	0.05	<0.01	97.92

the mineral of the qualitative composition Pt-Bi-Te is moncheite, (Pt, Pd)(Te, Bi)$_2$, its polymorphous equivalent merenskyite, or maslovite, (Pt, Pd)(Bi, Te). The mean size is 7.3 ± 9.0 μm but in some places large grains up to 150 μm × 10 μm were observed. Kotulskite, Pd(Te, Bi), was noted as 5.2 ± 2.9 μm sized grains. PGE-Bi-tellurides have a typical appearance of elongated, needle- or worm-like grains. In most instances they are intergrown with silicates and/or pentlandite, only rarely with chalcopyrite or pyrrhotite.

Platinum-iron-alloy is, with 387 grains, by far the most abundant PGM. On the basis of its composition, which approximates Pt_3Fe, it is most probably isoferroplatinum; an unequivocal identification would require, the determination of the crystal structure (Cabri and Feather, 1975). This mineral usually occurs as euhedral, angular, and in places, ragged grains, on average 7.7 ± 6.1 μm in size. The isoferroplatinum was observed as clusters of over 100 single grains at the edges of sulfide aggregates (Fig. 3*c–f*). A strong preference to pyrrhotite was noted with as much as 62% of the counted Pt-Fe alloy grains being completely enclosed by pyrrhotite, 10% were found hosted by pentlandite and 7% at pentlandite-pyrrhotite grain boundaries. Only very rarely are the Pt-Fe alloy grains completely surrounded by silicates or intergrown with magnetite. They are never associated with chalcopyrite. Analogous to Fig. 3*a*, although less apparent due to the low brightness and contrast setting, the pyrrhotite host in proximity to isoferroplatinum shows slightly brighter exsolution lamellae of troilite (best seen in Fig. 3*c* and *d*).

In addition, one grain of rustenburgite or atokite, (Pt, Pd)$_3$Sn, with an ECD of 16.9 μm was noted, as well as 14 grains of electrum, (Au,Ag). The grain size (ECD) of electrum was found to be 8.0 ± 19.3 μm (median ECD 2.5 μm). One grain has an exceptional size of 110 μm × 45 μm. In contrast to the PGM, electrum is typically completely enclosed by silicates in sulfide-free domains. In only two cases, AuAg was observed at the chalcopyrite-amphibole/plagioclase interface. Electrum grains, where enclosed by rustenburgite, contain considerable amounts of iridium. Two small grains (ECD of 1.1 μm and 2.0 μm) found in pentlandite, with a composition of (ReOsIrPtFe)(AsS), are probably a polyphase of rheniite (ReS_2) and irarsite ((Ir,Pt)AsS).

Interpretation and discussion

The mineralogy and texture of the investigated samples from the Rustenburg Mine, with specific

https://doi.org/10.1180/minmag.2016.080.055 Published online by Cambridge University Press

reference to PGM, are in broad agreement with previous studies (e.g. Vermaak and Hendriks, 1976; Kingston and El-Dosuky, 1982; Viljoen and Hieber, 1986; Kinloch and Peyerl, 1990; Schouwstra *et al.*, 2000; Cawthorn *et al.*, 2002; Li *et al.*, 2004; Godel *et al.*, 2007; Vukmanovic *et al.*, 2013). The sulfide-PGM association is clearly a ubiquitous feature of the Merensky Reef and we take this as evidence that PGE were initially taken up by immiscible sulfide droplets. At least some needle-like inclusions of laurite in pentlandite suggest that these exsolved from the sulfide at quite low temperatures. Establishing the origin of PGE-sulfides, -arsenides and -tellurides, be they high- or low-temperature phenomena, is beyond the scope of this study and has been discussed in numerous other studies (e.g. Brenan and Andrews, 2001; Helmy *et al.*, 2007; Finnigan *et al.*, 2008; Holwell and McDonald, 2010; Helmy *et al.*, 2013, and references therein). Of interest here is the proportion of isoferroplatinum, which was found in this study to be much greater than reported previously. This may be attributed to small-scale variations in modal mineralogy. Similar accumulations of isoferroplatinum hosted by pyrrhotite within the Merensky Reef were also reported by Vermaak and Hendriks (1976), Kinloch (1982), Kingston and El-Dosuky (1982) as well as Godel *et al.* (2007). Here, we would like to draw the attention, however, to these extraordinary PGM microstructures (Fig. 3*c–f*).

Pyrrhotite is known to host variable amounts (below 1 ppm up to tens of ppm) of Pt (e.g. Makovicky *et al.*, 1986; Ballhaus and Ulmer, 1995; Ballhaus and Ryan, 1995; Godel *et al.*, 2007; Osbahr *et al.*, 2013), which is explained by the substitution of Pt for Fe-vacancies in the $Fe_{1-x}S$ crystal lattice (Ballhaus and Ulmer, 1995). It has also been shown experimentally that the solubility of Pt decreases with increasing Fe/S ratio of the pyrrhotite (Makovicky *et al.*, 1990; Li *et al.*, 1996; Majzlan *et al.*, 2002). Thus, stoichiometric FeS (troilite) is not able to incorporate any PGE (Majzlan *et al.*, 2002; Peregoedova *et al.*, 2004). Consequently, PGE-bearing pyrrhotite of the Merensky Reef could have released PGE in the course of desulfurization. In our opinion, this is reflected well by the observed intergrowths of isoferroplatinum with troilite and Fe-rich pyrrhotite (Fig. 3): pyrrhotite lost S by processes discussed below, thus becoming enriched in Fe and attaining, in places, troilite composition. Platinum, initially hosted by the sulfide, exsolved into discrete phases – in this case a Pt-Fe-alloy.

Some authors (e.g. Hiemstra, 1979; Merkle, 1992; Borisov and Palme 1997; Ballhaus and Sylvester, 2000; Maijzlan *et al.*, 2002; Kamenetsky *et al.*, 2015) have suggested, however, that Pt-Fe-alloys can also crystallize directly, prior to sulfide saturation or together with sulfides, chromite or silicates, from a PGE-saturated silicate melt. Such a process is considered unlikely in the case of the samples studied for the following reason. As evident in Fig. 3*f*, isoferroplatinum has a preferred association with pyrrhotite rather than with pentlandite, even within polyphase sulfide aggregates. Such a co-accumulation of a large proportion of Pt-Fe only with pyrrhotite but not with other sulfides seems hardly explicable by direct Pt-Fe crystallization from a silicate melt. Instead, the observed spatial association is more easily explained by isoferroplatinum having formed after the recrystallization of the monosulfide solid solution to pentlandite and pyrrhotite at temperatures below ~650°C (Holwell and McDonald, 2010).

It has been suggested that S loss affected the Merensky and UG2 reefs. For example, Naldrett and Lehmann (1988), following the observations made by Gain (1985), have shown that non-stoichiometric chromite that crystallizes from a basaltic magma interacted with surrounding sulfides. In this case, Fe is taken up by the chromite in order to fill vacancies and S leaves the system. Although this process has been a popular explanation for the high metal/S ratios in the Merensky and UG2 reefs, it seems unlikely to be of major significance in the samples investigated for two reasons. First, the (isoferroplatinum-) pyrrhotite-troilite intergrowths are never observed in the vicinity of chromite, and second, the process described by Naldrett and Lehmann (1988) should not produce Fe-rich sulfides, as noted in the analysed samples, but Ni- and Cu-rich sulfides.

Another possibility of desulfurization in layered intrusions is the interaction with S-undersaturated fluids (Boudreau, 1988; Peregoedova *et al.*, 2004, 2006; Li and Ripley, 2006; Godel and Barnes, 2008). This notion is favoured and agrees well with our observation of hydrothermal alteration and the isoferroplatinum-pyrrhotite-troilite intergrowths at the edges of sulfide aggregates, as it is probable that alteration and desulfurization predominantly affected the sulfide-silicate grain boundaries. We therefore suggest the following sequence of processes to have led to the observed mineral associations: crystallization of the rocks below the Merensky Unit produced a residual CO_2 (and Cl?)-bearing hydrous fluid. The sulfur-deficient fluid

https://doi.org/10.1180/minmag.2016.080.055 Published online by Cambridge University Press

ascended, perhaps squeezed by tectonics or voluminous magma influxes above, and interacted with the Merensky Reef. The resulting metasomatism led to the replacement of primary magmatic minerals and to the partial desulfurization of (orthomagmatic) PGE-bearing sulfides. As already suggested, this is believed to have triggered the formation of isoferroplatinum and, in some cases, the liberation of PGM from their sulfide host. Similarly to the chromatographic model of Boudreau and Meurer (1999) and Willmore *et al.* (2000), the fluid could have re-dissolved into the interstitial melt or magma at the top of the cumulate pile – a process that would explain the unaltered character of the hanging wall and the upwards increase in f_{S_2} (implied by troilite and magnetite found in the reef, and pyrite in the hanging wall).

Some studies (Kinloch, 1982; Kinloch and Peyerl, 1990) have assumed that the predominance of Pt-Fe-alloys over Pt-sulfides, such as cooperite/braggite, could be the result of high f_{O_2} and low f_{S_2} within, or in proximity to, potholes and perhaps this might also apply, locally, to the Normal Merensky Reef facies. For various reasons, Ballhaus (1988) and Boudreau (1992) further suggested that potholes represent volatile/fluid escape structures, which were released from the underlying cumulates. Our observations seem to support this hypothesis and conform to previous hypotheses that PGM, especially Pt-Fe-alloys, could also be a subsolidus crystallization product (Ballhaus and Ulmer, 1995).

Conclusions

Detailed petrographic and mineralogical studies of the Rustenburg thin reef facies of the Merensky Reef (Normal Merensky Reef facies) make it possible to draw several conclusions regarding its mineralogy and genesis:

(1) A larger than expected quantity of hydrous silicates (serpentine, chlorite, epidote, talc, tremolite) but also fine-grained carbonates and some magnetite exist in the Normal Merensky Reef facies. These alteration minerals tend to replace magmatic minerals (pyroxene, plagioclase, sulfides) in the reef but are absent in the hanging wall.

(2) Isoferroplatinum (Pt_3Fe) is the dominant PGM, instead of PGE-sulfides, -tellurides and -arsenides, as usually known for this Merensky Reef type. A Pt-Fe-alloy dominated facies is known from (hydrothermal influenced?) potholes and other cross-cutting structures.

(3) Troilite (stoichiometric FeS) was found as exsolution lamellae in Fe-rich pyrrhotite ($Fe_{1-x}S$). Troilite is absent in the hanging wall, where pyrite (FeS_2) is part of the paragenesis.

(4) Polyphase interstitial sulfide aggregates are visibly fragmented and hydrothermally altered, predominantly at their margins. Satellite grains of PGM that were originally hosted by sulfides, are now isolated (i.e. completely enclosed by secondary minerals).

(5) Isoferroplatinum is intergrown with troilite and Fe-rich pyrrhotite, always located at the edges of sulfide aggregates and in contact with secondary gangue minerals. Such an assemblage has only been recognized in the most intensely hydrothermally modified domains of our samples. The rare association of Pt-Fe-alloy with magnetite is also noteworthy.

(6) Textural evidence suggests that isoferroplatinum formed at relatively low temperatures, i.e. after the transition of a monosulfide solid solution into pentlandite and pyrrhotite.

On the basis of our observations and published data (Kinloch, 1982; Kinloch and Peyerl, 1990; Li *et al.*, 2004; Li and Ripley, 2006; Godel and Barnes, 2008), we conclude that the Merensky Reef has undergone local metasomatism, not only at potholes (fluid escape structures?), but also away from these zones of disturbance. Sulfur-undersaturated, CO_2-bearing hydrous fluids, perhaps released from the underlying, consolidating cumulate pile, probably migrated upwards and led to the observed alteration and partial desulfurization of PGE-bearing sulfides. Another consequence was the formation of troilite, Fe-rich pyrrhotite and some magnetite, as well as the exsolution of isoferroplatinum from an initial Pt-bearing pyrrhotite. Due to the strong spatial association, we suggest that all PGE were taken up originally by an immiscible sulfide melt. This notion is similar to the conclusions drawn by Godel and Barnes (2008) for the J-M Reef (Stillwater Complex), on the basis of isoferroplatinum-pyrrhotite/pentlandite-magnetite intergrowths and the low whole-rock S/Se ratio, which indicates a substantial loss of sulfur.

Overall, our observations emphasize the significance of fluids and hydrothermal alteration, not for the primary PGE-mineralization but for the local reconstitution of the ore minerals into the current PGM mineralogy and textures. Even in areas that were not affected by pothole formation, PGM assemblages and textures should not *a priori* be regarded as primary and a late-magmatic fluid-induced open system behaviour should be considered. Thus we concur with Li *et al.* (2004, p.183)

https://doi.org/10.1180/minmag.2016.080.055 Published online by Cambridge University Press

that "the effects of secondary hydrothermal alteration […] in the UG2 and Merensky Reef may be more significant than previously thought and should not be ignored in genetic modelling".

Acknowledgements

The authors thank U. Schüßler and P. Späthe for assistance with the electron microprobe and preparation of thin sections, respectively. The samples analysed all form part of the collection of the Mineralogical Museum of the University of Wuerzburg, where they are stored and curated. R. Voordouw and an anonymous reviewer are thanked for their constructive and helpful comments on the original manuscript and B. O'Driscoll for the editorial handling.

References

Ballhaus, C.G. (1988) Potholes of the Merensky Reef at Brakspruit Shaft, Rustenburg Platinum Mines: Primary disturbances in the magmatic stratigraphy. *Economic Geology*, **83**, 1140–1158.

Ballhaus, C.G. and Ryan, C.G. (1995) Platinum-group elements in the Merensky reef. I. PGE in solid solution in base metal sulphides and the down-temperature equilibration history of Merensky ores. *Contributions to Mineralogy and Petrology*, **122**, 241–251.

Ballhaus, C.G. and Stumpfl, E.F. (1986) Sulfide and platinum mineralisation in the Merensky Reef: evidence from hydrous silicates and fluid inclusions. *Contributions to Mineralogy and Petrology*, **94**, 193–204.

Ballhaus, C.G. and Sylvester, P. (2000) Noble metal enrichment processes in the Merensky Reef, Bushveld Complex. *Journal of Petrology*, **41**, 545–561.

Ballhaus, C.G. and Ulmer, P. (1995) Platinum-group elements in the Merensky reef: II. Experimental solubilities of platinum and palladium in Fe1–xS from 950 to 450°C under controlled f_{S_2} and f_{H_2}. *Geochimica et Cosmochimica Acta*, **59**, 4881–4888.

Barnes, S-J. and Maier, W.D. (2002) Platinum-group element distributions in the Rustenberg Layered Suite of the Bushveld Complex, South Africa. pp. 431–458 in: *The Geology, Geochemistry, Mineralogy and Mineral Beneficiation of Platinum-Group Elements* (L.J. Cabri, editor). Canadian Institute of Mining, Metallurgy and Petroleum, Special Volume 54, Montreal, Quebec, Canada.

Borisov, A. and Palme, H. (1997) Experimental determination of the solubility of platinum in silicate melts. *Geochimica et Cosmochimica Acta*, **61**, 4349–4357.

Boudreau, A.E. (1988) Investigations of the Stillwater Complex: VI. The role of volatiles in the petrogenesis of the J-M Reef, Minneapolis adit section. *The Canadian Mineralogist*, **26**, 193–208.

Boudreau, A.E. (1992) Volatile fluid overpressure in layered intrusions and the formation of potholes. *Australian Journal of Earth Sciences*, **39**, 277–287.

Boudreau, A.E. (2008) Modelling the Merensky Reef, Bushveld Complex, Republic of South Africa. *Contributions to Mineralogy and Petrology*, **156**, 431–437.

Boudreau, A.E. and Meurer, W.P. (1999) Chromatographic separation of the platinum-group elements, gold, base metals and sulfur during degassing of a compacting and solidifying igneous crystal pile. *Contributions to Mineralogy and Petrology*, **134**, 174–185.

Boudreau, A.E. and McCallum, I.S. (1992) Concentration of platinum-group elements by magmatic fluids in layered intrusions. *Economic Geology*, **87**, 1830–1848.

Brenan, J.M. and Andrews, D. (2001) High-temperature stability of laurite and Ru-Os-Ir alloy and their role in PGE fractionation in mafic magmas. *The Canadian Mineralogist*, **39**, 341–360.

Cabri, L.J. and Feather, C.E. (1975) Platinum–iron alloys: a nomenclature based on a study of natural and synthetic alloys. *The Canadian Mineralogist*, **13**, 117–126.

Campbell, I.H., Naldrett, A.J. and Barnes, S.-J. (1983) A model for the origin of the platinum-rich sulfide horizons in the Bushveld and Stillwater Complexes. *Journal of Petrology*, **24**, 133–165.

Cawthorn, R.G. (1999) Platinum-group element mineralization in the Bushveld Complex – a critical assessment of geochemical models. *South African Journal of Geology*, **102**, 268–281.

Cawthorn, R.G. (2005) Pressure fluctuations and the formation of the PGE rich Merensky and chromitite reefs, Bushveld Complex. *Mineralium Deposita*, **40**, 231–235.

Cawthorn, R.G. (2010) Geological interpretations from the PGE distribution in the Bushveld Merensky and UG2 chromitite reefs. *The 4th International Platinum Conference, Platinum in transition 'Boom or Bust'*. The Southern African Institute of Mining and Metallurgy, Abstract pp. 57–70.

Cawthorn, R.G. and Boerst, K. (2006) Origin of the pegmatitic pyroxenite in the Merensky Unit, Bushveld Complex, South Africa. *Journal of Petrology*, **47**, 1509–1530.

Cawthorn, R.G. and Walraven, F. (1998) Emplacement and crystallization time for the Bushveld Complex. *Journal of Petrology*, **39**, 1669–1687.

Cawthorn, R.G. and Webb, S.J. (2013) Cooling of the Bushveld Complex, South Africa: implications for paleomagnetic reversals. *Geology*, **41**, 687–690.

Cawthorn, R.G., Lee, C.A., Schouwstra, R.P. and Mellowship, P. (2002) Relationship between PGE and PGM in the Bushveld Complex. *The Canadian Mineralogist*, **40**, 311–328.

https://doi.org/10.1180/minmag.2016.080.055 Published online by Cambridge University Press

Cawthorn, R.G., Barnes, S.-J., Ballhaus, C.G. and Malitch, K.N. (2005) Platinum group element, chromium, and vanadium deposits in mafic and ultramafic rocks. *Economic Geology* [SEG 100th Anniversary Volume], 215–249.

Eales, H.V. and Cawthorn, R.G. (1996) The Bushveld Complex. pp. 181–230 in: *Layered Intrusions* (R.G. Cawthorn, editor). Developments in Petrology, 15. Elsevier, Amsterdam, Netherlands.

Finnigan, G.S., Brenan, J.M., Mungall, J.E. and McDonough, W.F. (2008) Experiments and models bearing on the role of chromite as a collector of platinum group minerals by local reduction. *Journal of Petrology*, **49**, 1647–1665.

Gain, S.B. (1985) The geological setting of the platiniferous UG2 chromitite layer on the farm Maandagshoek, eastern Bushveld Complex. *Economic Geology*, **77**, 1395–1404.

Godel, B. and Barnes, S.-J. (2008) Image analysis and composition of platinum-group minerals in the J-M Reef, Stillwater Complex. *Economic Geology*, **103**, 637–651.

Godel, B., Barnes, S.-J. and Maier, W.D. (2007) Platinum-group elements in sulphide minerals, platinum-group minerals, and whole-rocks of the Merensky Reef (Bushveld Complex, South Africa): implications for the formation of the reef. *Journal of Petrology*, **48**, 1569–1604.

Hatton, C.J. (1995) Mantle plume origin for the Bushveld and Ventersdorp magmatic provinces. *Journal of African Earth Sciences*, **21**, 571–577.

Helmy, H.M., Ballhaus, C.G., Berndt, J., Bockrath, C. and Wohlgemuth-Ueberwasser, C. (2007) Formation of Pt, Pd and Ni tellurides: experiments in sulfide-telluride systems. *Contributions to Mineralogy and Petrology*, **153**, 577–591.

Helmy, H.M., Ballhaus, C.G., Fonseca, R.O.C., Wirth, R., Nagel, T. and Tredoux, M. (2013) Noble metal nanoclusters and nanoparticles precede mineral formation in magmatic sulphide melts. *Nature Communications*, **4**, 2405.

Hiemstra, S.A. (1979) The role of collectors in the formation of the platinum deposits in the Bushveld Complex. *The Canadian Mineralogist*, **17**, 469–482.

Holwell, D.A. and McDonald, I. (2010) A review of the behaviour of platinum group elements within natural magmatic sulfide ore systems. *Platinum Metals Review*, **54**, 26–36.

Hutchinson, D., Foster, J., Prichard, H. and Gilbert, S. (2015) Concentration of particulate platinum-group minerals during magma emplacement; a case study from the Merensky Reef, Bushveld Complex. *Journal of Petrology*, **56**, 113–159.

Junge, M., Wirth, R., Oberthür, T., Melcher, F. and Schreiber, A. (2015) Mineralogical siting of platinum-group elements in pentlandite from the Bushveld Complex, South Africa. *Mineralium Deposita*, **50**, 41–54.

Kamenetsky, V.S., Park, J.-W., Mungall, J.E., Pushkarev, E.V., Ivanov, A.V., Kamenetsky, M.B. and Yaxley, G. M. (2015) Crystallization of platinum-group minerals from silicate melt: Evidence from Cr-spinel–hosted inclusions in volcanic rocks. *Geology*, **43**, 903–906.

Kanitpanyacharoen, W. and Boudreau, A.E. (2013) Sulfide-associated mineral assemblages in the Bushveld Complex, South Africa: platinum-group element enrichment by vapor refining by chloride–carbonate fluids. *Mineralium Deposita*, **48**, 193–210.

Kingston, G.A. and El-Dosuky, B.T. (1982) A contribution on the platinum-group mineralogy of the Merensky Reef at the Rustenburg platinum mine. *Economic Geology*, **77**, 1367–1384.

Kinloch, E.D. (1982) Regional trends in the platinum-group mineralogy of the critical zone of the Bushveld Complex, South Africa. *Economic Geology*, **77**, 1328–1347.

Kinloch, E.D. and Peyerl, W. (1990) Platinum-group minerals in various rock types of the Merensky Reef: genetic implications. *Economic Geology*, **85**, 537–555.

Kruger, F.J. (2005) Filling the Bushveld Complex magma chamber: lateral expansion, roof and floor interaction, magmatic unconformities, and the formation of giant chromitite, PGE and Ti-V-magnetite deposits. *Mineralium Deposita*, **40**, 451–472.

Lee, C.A. (1996) A review of mineralisation in the Bushveld Complex and some other layered intrusions. pp. 103–146 in: *Layered Intrusions* (R.G. Cawthorn, editor). Developments in Petrology, 15. Elsevier, Amsterdam, Netherlands.

Letts, S., Torsvik, T.H., Webb, S.J. and Ashwal, L.D. (2009) Palaeomagnetism of the 2054 Ma Bushveld Complex (South Africa): implications for emplacement and cooling. *Geophysical Journal International*, **179**, 850–872.

Li, C. and Ripley, E.M. (2006) Formation of Pt-Fe alloy by desulfurization of Pt-sulfide in the J-M Reef of the Stillwater Complex, Montana. *The Canadian Mineralogist*, **44**, 895–903.

Li, C., Barnes, S.-J., Makovicky, E., Rose-Hansen, J. and Makovicky, M. (1996) Partitioning of nickel, copper, iridium, rhodium, platinum, and palladium between monosulfide solid solution and sulfide liquid: effects of composition and temperature. *Geochimica et Cosmochimica Acta*, **60**, 1231–1238.

Li, C., Ripley, E.M., Merino, E. and Maier, W.D. (2004) Replacement of base metal sulfides by actinolite, epidote, calcite, and magnetite in the UG2 and Merensky Reef of the Bushveld Complex, South Africa. *Economic Geology*, **99**, 173–184.

Li, C., Ripley, E.M., Oberthür, T., Miller, J.D. Jr. and Joslin, G.D. (2008) Textural, mineralogical and stable

https://doi.org/10.1180/minmag.2016.080.055 Published online by Cambridge University Press

isotope studies of hydrothermal alteration in the main sulfide zone of the Great Dyke, Zimbabwe and the precious metals zone of the Sonju Lake Intrusion, Minnesota, USA. *Mineralium Deposita*, **43**, 97–110.

Maier, W.D., Barnes, S.-J. and Groves, D.I. (2013) The Bushveld Complex, South Africa: formation of platinum-palladium, chrome- and vanadium-rich layers via hydrodynamic sorting of a mobilized cumulate slurry in a large, relatively slowly cooling, subsiding magma chamber. *Mineralium Deposita*, **48**, 1–56.

Majzlan, J., Makovicky, M., Makovicky, E. and Rose-Hansen, J. (2002) The system Fe–Pt–S at 1100 °C. *The Canadian Mineralogist*, **40**, 509–517.

Makovicky, E., Karup-Møller, S., Makovicky, M. and Rose-Hansen, J. (1990) Experimental studies on the phase systems Fe–Ni–Pd–S and Fe–Pt–Pd–As–S applied to PGE deposits. *Mineralogy and Petrology*, **42**, 307–319.

Makovicky, M., Makovicky, E. and Rose-Hansen, J. (1986) Experimental studies on the solubility and distribution of platinum-group elements in base metal sulphides in platinum deposits. pp. 415–425 in: *Metallogeny of Basic and Ultrabasic Rocks* (M.J. Gallagher, R.A. Ixer, C.R. Neary and H.M. Prichard, editors). Institution of Mining and Metallurgy London, UK.

Merkle, R.K.W. (1992) Platinum-group minerals in the middle group of chromitite layers at Marikana, western Bushveld Complex: indications for collection mechanism and postmagmatic modification. *Canadian Journal of Earth Science*, **29**, 209–221.

Naldrett, A.J. and Lehmann, J. (1988) Spinel Non-stoichiometry as the Explanation for Ni-, Cu- and PGE-enriched Sulphides in Chromitites. pp. 113–143 in: *Geo-Platinum 87* (H.M. Prichard, P.J. Potts, J.F.W. Bowles, and S.J. Cribb, editors). Elsevier, London, UK.

Naldrett, A.J. and von Gruenewaldt, G. (1989) The association of PGE with chromitite in layered intrusions and ophiolite complexes. *Economic Geology*, **84**, 180–187.

Naldrett, A.J., Kinnaird, J., Wilson, A. and Chunnett, G. (2008) Concentration of PGE in the earth's crust with special reference to the Bushveld Complex. *Earth Science Frontiers*, **15**, 264–297.

Naldrett, A.J., Wilson, A., Kinnaird, J. and Chunnett, G. (2009) PGE tenor and metal ratios within and below the Merensky Reef, Bushveld Complex: implications for its genesis. *Journal of Petrology*, **50**, 625–659.

Naldrett, A.J., Kinnaird, J., Wilson, A., Yudovskaya, M. and Chunnett, G. (2011) Genesis of the PGE-enriched Merensky Reef and chromitite seams of the Bushveld Complex. Pp. 235–296 in: *Magmatic Ni-Cu and PGE Deposits* (C. Li and E.M. Ripley, editors). Reviews in Economic Geology, 17, Littleton, Colorado, USA.

Osbahr, I., Klemd, R., Oberthür, T., Brätz, H. and Schouwstra, R.P. (2013) Platinum-group element distribution in base-metal sulfides of the Merensky Reef from eastern and western Bushveld Complex, South Africa. *Mineralium Deposita*, **48**, 211–232.

Peregoedova, A., Barnes, S.-J. and Baker, D.R. (2004) The formation of Pt–Ir alloys and Cu–Pd-rich sulfide melts by partial desulfurization of Fe–Ni–Cu sulfides: results of experiments and implications for natural systems. *Chemical Geology*, **208**, 247–264.

Peregoedova, A., Barnes, S.-J. and Baker, D.R. (2006) An experimental study of mass transfer of platinum-group elements, gold, nickel and copper in sulfur-dominated vapour at magmatic temperatures. *Chemical Geology*, **235**, 59–75.

Rose, D., Viljoen, F., Knoper, M. and Rajesh, H. (2011) Detailed assessment of platinum-group minerals associated with chromitite stringers in the Merensky Reef of eastern Bushveld Complex, South Africa. *The Canadian Mineralogist*, **49**, 1385–1396.

SACS [South African Committee for Stratigraphy] (1980) Stratigraphy of South Africa. Part 1. in: *Lithostratigraphy of the Republic of South Africa* (L.E. Kent, editor). Geological Survey of South Africa Handbook **8**. Pretoria, South Africa.

Schönberg, R., Kruger, F.J., Nägler, T.F., Meisel, T. and Kramers, J.D. (1999) PGE enrichment in chromitite layers and the Merensky Reef of the western Bushveld Complex; a Re–Os and Rb–Sr isotope study. *Earth and Planetary Science Letters*, **172**, 49–64.

Schouwstra, R.P., Kinloch, E.D. and Lee, C.A. (2000) A short geological review of the Bushveld Complex. *Platinum Metals Review*, **44**, 33–39.

Scoates, J.S., Wall, C.J., Friedman, R. and Chamberlain, K. (2011) Revisiting the age of the Merensky Reef, Bushveld Complex. *Mineralogical Magazine*, **75**, 1831.

Scoon, R.N. and Mitchell, A.A. (2011) The principal geological features of the Mooihoek platiniferous dunite pipe, eastern limb of the Bushveld Complex, and similarities with replaced Merensky Reef at the Amandelbult Mine, South Africa. *South African Journal of Geology*, **114**, 15–40.

Tredoux, M., Lindsay, N.M., Davies, G. and McDonald, I. (1995) The fractionation of platinum-group elements in magmatic systems, with the suggestion of a novel causal mechanism. *South African Journal of Geology*, **98**, 157–167.

U.S. Geological Survey (2015) Mineral commodity summaries 2015. *U.S. Geological Survey*, 196 pp.

Vermaak, C.F. and Hendriks, L.P. (1976) A review of the mineralogy of the Merensky Reef, with specific reference to new data on the precious metal mineralogy. *Economic Geology*, **71**, 1244–1269.

Viljoen, M.J. and Hieber, R. (1986) The Rustenburg Section of Rustenburg Platinum Mines Limited, with reference to

https://doi.org/10.1180/minmag.2016.080.055 Published online by Cambridge University Press

the Merensky Reef. Pp. 1107–1134 in: *Mineral deposits of southern Africa* (C.R. Anhaeusser and S. Maske, editors). Geological Society of South Africa Special Publication, **2**. Johannesburg, South Africa.

Vukmanovic, Z., Barnes, S.-J., Reddy, S.M., Godel, B. and Fiorentini, M.L. (2013) Morphology and microstructure of chromite crystals in the Merensky Reef (Bushveld Complex, South Africa). *Contributions to Mineralogy and Petrology*, **165**, 1031–1050.

Webb, S.J., Ashwal, L.D. and Cawthorn, R.G. (2011) Continuity between eastern and western Bushveld Complex, South Africa, confirmed by xenoliths from kimberlite. *Contributions to Mineralogy and Petrology*, **162**, 101–107.

Willmore, C.C., Boudreau, A.E. and Kruger, F.J. (2000) The halogen geochemistry of the Bushveld Complex, Republic of South Africa: implications for chalcophile element distribution in the Lower and Critical zones. *Journal of Petrology*, **41**, 1517–1539.

Willmore, C.C., Boudreau, A.E., Spivack, A. and Kruger, F.J. (2002) Halogens of Bushveld Complex, South Africa δ^{37}Cl and Cl/F evidence for hydration melting of the source region in a back-arc setting. *Chemical Geology*, **182**, 503–511.

Xiao, Z. and Laplante, A.R. (2004) Characterizing and recovering the platinum group minerals – a review. *Minerals Engineering*, **17**, 961–979.

Zeh, A., Ovtcharova, M., Wilson, A.H. and Schaltegger, U. (2015) The Bushveld Complex was emplaced and cooled in less than one million years – results of zirconology and geotectonic implications. *Earth and Planetary Science Letters*, **418**, 103–114.

https://doi.org/10.1180/minmag.2016.080.055 Published online by Cambridge University Press